

Article

Comparison of Chemiluminescence Enzyme Immunoassay (Cl-ELISA) with Colorimetric Enzyme Immunoassay (Co-ELISA) for Imidacloprid Detection in Vegetables

Rongqi Zhai ^{1,†}, Ge Chen ^{1,†}, Guangyang Liu ¹, Xiaodong Huang ¹, Xiaomin Xu ¹, Lingyun Li ¹, Yanguo Zhang ¹, Donghui Xu ^{1,*} and A. M. Abd El-Aty ^{2,3} 

¹ Key Laboratory of Vegetables Quality and Safety Control, Laboratory of Quality & Safety Risk Assessment for Vegetable Products, Ministry of Agriculture and Rural Affairs, Institute of Vegetables and Flowers, Chinese Academy of Agricultural Sciences, Beijing 100081, China

² Department of Pharmacology, Faculty of Veterinary Medicine, Cairo University, Giza 12211, Egypt

³ Department of Medical Pharmacology, Faculty of Medicine, Atatürk University, 25240 Erzurum, Turkey

* Correspondence: xudonghui@caas.cn; Tel.: +86-10-8210-6963

† These authors contributed equally to this work.

Abstract: Imidacloprid is one of the most commonly used insecticides for managing pests, thus, improving the quality and yield of vegetables. The abuse/misuse of imidacloprid contaminates the environment and threatens human health. To reduce the risk, a colorimetric enzyme-linked immunoassay assay (Co-ELISA) and chemiluminescence enzyme-linked immunoassay assay (Cl-ELISA) were established to detect imidacloprid residues in vegetables. The linear range of Co-ELISA ranged between 1.56 µg/L and 200 µg/L with a limit of detection (LOD) of 1.56 µg/L. The values for Cl-ELISA were 0.19 µg/L to 25 µg/L with an LOD of 0.19 µg/L, which are lower than those of Co-ELISA. Fortifying Chinese cabbage, cucumber, and zucchini with imidacloprid at 10, 50, and 100 µg/L yielded recoveries between 81.7 and 117.6% for Co-ELISA and at 5, 10, and 20 µg/L yielded recoveries range from 69.7 to 120.6% for Cl-ELISA. These results indicate that Cl-ELISA has a high sensitivity and a rapid detection time, saving cost (antigen and antibody concentrations) and serving as a more efficient model for the rapid detection of imidacloprid residue.

Keywords: imidacloprid; colorimetric assay; chemiluminescent assay; enzyme-linked immunoassay



Citation: Zhai, R.; Chen, G.; Liu, G.; Huang, X.; Xu, X.; Li, L.; Zhang, Y.; Xu, D.; Abd El-Aty, A.M. Comparison of Chemiluminescence Enzyme Immunoassay (Cl-ELISA) with Colorimetric Enzyme Immunoassay (Co-ELISA) for Imidacloprid Detection in Vegetables. *Foods* **2023**, *12*, 196. <https://doi.org/10.3390/foods12010196>

Academic Editor: Thierry Noguere

Received: 24 November 2022

Revised: 22 December 2022

Accepted: 26 December 2022

Published: 1 January 2023



Copyright: © 2023 by the authors. Licensee MDPI, Basel, Switzerland. This article is an open access article distributed under the terms and conditions of the Creative Commons Attribution (CC BY) license (<https://creativecommons.org/licenses/by/4.0/>).

1. Introduction

Imidacloprid (IMI), a neonicotinoid insecticide, is widely used for pest control in agriculture, ensuring the yield and quality of vegetables [1]. Although IMI is highly efficient for pest control, its misuse and abuse are expected to seriously threaten the ecosystem and public health [2,3]. IMI fails to degrade completely, resulting in long persistence [4]. Long-term exposure to IMI causes neurological damage, which poses a great risk to human health [5,6]. Hence, a sensitive analysis of IMI residues in foods is required to reduce health and environmental risks from hazardous materials.

Many instrumental methods, such as liquid chromatography (LC) [7], liquid chromatography–tandem mass spectrometry (LC–MS/MS) [8], and gas chromatography–tandem mass spectrometry (GC–MS/MS) [9], have been used to determine IMI residues. However, these methods are costly, complex, and time-consuming [10]. Rapid detection methods (such as immunoassays [11,12], aptamer methods [13], and electrochemical sensor methods [14,15]) with high sensitivity, simple operation, and low cost have been developed to overcome the shortcomings of these methods. In immunoassays, antibodies have the property of highly sensitive molecular recognition [16]. Enzyme-linked immunoassay (ELISA), as one of the immunoassays for the rapid evaluation of neonicotinoid insecticides, consists of two main formats: direct competitive ELISA (DC-ELISA) and indirect competitive ELISA

(IC-ELISA) [17–19]. IC-ELISA is widely used to detect pesticide residues because of its advantages, such as high sensitivity, simplicity, simple pretreatment, and high throughput detection. For instance, Zhang et al. [20] used the colorimetric (Co) IC-ELISA method to determine IMI residues with an LOD of 0.025 mg/L, showing high sensitivity and stability. Yue et al. [21] also used Co-IC-ELISA to determine organophosphate pesticides in agricultural products, obtaining an LOD for methyl parathion of 1.94 ng/mL. The method yielded favorable recoveries of 84.16–106.96% at a low spiking level. Compared to colorimetric assays, chemiluminescence, as a highly sensitive detection method, is also used to rapidly detect IMI. For instance, Girotti et al. [22] used chemiluminescence to detect IMI in honey using IC-ELISA. They found that the LOD was 0.11 ng/mL. Similarly, Hu et al. [23] detected IMI based on IC-ELISA using chemiluminescence and obtained a low LOD of 0.637 ng/mL. Colorimetric and chemiluminescent assays based on IC-ELISA have been popularly used to detect IMI with low LOD. However, the LOD of the related IC-ELISA method can be further improved.

To improve the LOD of IC-ELISA, this study reports colorimetric and chemiluminescent IC-ELISAs for detecting IMI (Figure 1). Comparing the sensitivity, linear range, antigen–antibody ratio, and detection time of CI-ELISA and Co-ELISA provided an approach for selecting a detection assay. Finally, different sample preparations were developed for Co-ELISA and CI-ELISA, which further improved the sensitivity and recovery of Co-ELISA and CI-ELISA in vegetable samples, providing a reference for applying ELISAs.

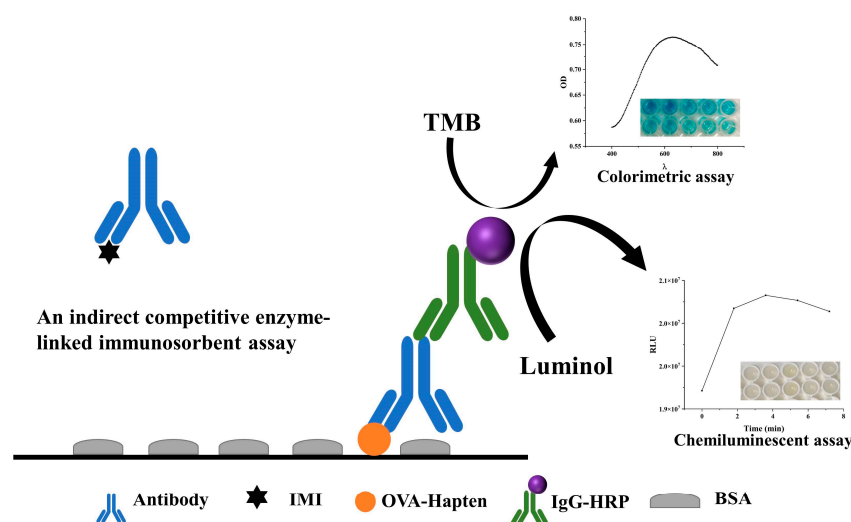


Figure 1. Illustration of the principle of Co-ELISA and CI-ELISA.

2. Materials and Methods

2.1. Chemicals and Reagents

Imidacloprid monoclonal antibody and ovalbumin-coated hapten (OVA-Hapten) were provided by Zhejiang University (Hangzhou, China). Peroxidase-conjugated AffiniPure goat antimouse IgG was purchased from Jackson ImmunoResearch Laboratories Inc. (West Grove, PA, USA). Imidacloprid standard (100 mg/kg) was procured from Beijing Manhage Bio-Technology Co., Ltd. (Beijing, China). Acetonitrile (chromatographic grade) was procured from Merck AG (Darmstadt, Germany). TMB (3,3',5,5'-Tetramethylbenzidine) single-component substrate solution, phosphate buffer saline tablets, and tris (hydroxymethyl) aminomethane were secured from Beijing Solarbio Science & Technology Co., Ltd. (Beijing, China). HRP-chemiluminescent reagents A and B were supplied by Beijing Keyuebio Technology Co., Ltd. (Beijing, China). Albumin (bovine serum) was obtained from Shanghai Yuanye Biotechnology Co., Ltd. (Shanghai, China). Tween 20 was acquired from Shanghai Macklin Biochemical Co., Ltd. (Shanghai, China). A 96-well opaque assay plate was obtained from Shanghai Jing An Biological Technology Co., Ltd. (Shanghai, China).

An immuno clear flat-bottom 96-well plate (item #439454#) was supplied by Thermo Fisher Scientific (Pittsburgh, PA, USA).

2.2. Optimization Parameters of the Assays

The experimental parameters (concentrations of antibody and antigen, concentration of BSA, organic solvent, and reaction time of chemiluminescence) were evaluated to improve the sensitivities of the CI-ELISA. Seven different combinations of antigen–antibody concentrations were screened (Table 1), and the corresponding IMI calibration curves were established to obtain the best combination of antigen–antibody concentrations. When the RLU_{max}/IC_{50} was greater than 5×10^5 , the minimum amount of antigen–antibody was desirable. The CI-ELISA detected IMI under various concentrations of BSA (0.5, 1, 2, 3, and 5%), implementing methanol to the final volume (1, 5, 10, 20, and 30%) in the IMI dilution, and chemiluminescence reaction times (from 0 to 20 min). The negative well RLU value, positive well RLU value, and N/P value (negative well RLU value/positive well RLU value) were used as evaluation criteria in the optimization scheme to select the best physicochemical parameters. For Co-ELISA, the optimal parameters of the Co-ELISA protocol were screened according to the chessboard titrations, including OD = 1 and cost savings [24]. The optimal combination was selected by comparing 32 combinations of antigen–antibody concentrations (Table 2).

Table 1. The optimal concentrations of antigen and antibody for CI-ELISA.

Antibody Concentration (mg/L)	OVA-Hapten Concentration (mg/L)			
	10		5	
	RLU_{max}/IC_{50}	R^2	RLU_{max}/IC_{50}	R^2
4	2.15×10^6	0.9676	-	-
2	7.56×10^5	0.9491	-	-
1	8.47×10^6	0.9266	1.49×10^6	0.9307
0.5	4.19×10^6	0.9582	6.24×10^6	0.9960
0.1	-	-	2.31×10^6	0.8743

Table 2. The optimal concentrations of antigen and antibody for Co-ELISA.

Antibody Dilution Times	OVA-Hapten Concentration (mg/L)			
	20	10	5	2.5
	2	1.8459	1.1196	0.7011
4	1.1879	0.8834	0.6110	0.5007
8	0.7198	0.6742	0.6787	0.5687
16	0.6613	0.6390	0.5700	0.4688
32	0.4950	0.6464	0.6006	0.5197
64	0.5268	0.4675	0.5115	0.5437
128	0.3867	0.4048	0.4691	0.4861
256	0.4395	0.4617	0.5157	0.3846

2.3. Sample Preparation

Method 1: Chinese cabbage, cucumber, and zucchini (purchased from local supermarkets) were selected as spiked samples. IMI standard concentrations (10, 50, and 100 $\mu\text{g/L}$) were used as fortification levels in homogenized samples (5 g) in 10 mL centrifuge tubes. The mixtures were stirred with 5 mL of methanol with manual shaking for 10 s and then left to extract for 30 min, followed by centrifugation at $8824 \times g$ (4 °C) for 15 min. Afterwards, 3 mL of supernatant was transferred to a 10 mL plastic centrifuge tube. Finally, 100 μL of supernatant was transferred to a 2 mL plastic tube, and 900 μL of PBS buffer solution (10 mM, pH = 4) was added to ensure a 10% ratio of methanol.

Method 2: Chinese cabbage, cucumber, and zucchini squash (purchased from local supermarkets) were selected as spiked samples. IMI standard concentrations (5, 10, and 20 $\mu\text{g/L}$) were used as spiking levels for homogenized samples (5 g) in 10 mL centrifuge tubes. The mixtures were stirred with 5 mL of methanol with manual shaking for 10 s and then left to extract for 30 min, followed by centrifugation at $8824 \times g$ (4°C) for 15 min. The entire supernatant was transferred to a 15 mL centrifuge tube, and water was added to adjust the volume to 10 mL. Finally, 200 μL of the supernatant was transferred to a 2 mL plastic tube, and 800 μL of PBS buffer solution (10 mM, $\text{pH} = 4$) was added to ensure a 10% ratio of methanol.

2.4. Co-ELISA Establishment

A 100 μL /well OVA-Hapten (10 mg/L) in PBS (10 mM, $\text{pH} 7.4$) was coated on an immuno clear flat-bottom 96-well plate for 2 h. The plates were then washed three times using PBST, followed by adding a BSA (300 μL /well) blocker for 1 h. After washing three times with PBST, IMI (50 μL /well) dissolved in 10% MeOH–PBS (10 mM, $\text{pH} 7.4$) and antibody (2 mg/L, 50 μL /well) diluted with tris (50 mM, $\text{pH} 7.4$) were added and incubated for 2 h on a blocked plate. After washing, 100 μL /well of diluted (1/1000) goat antimouse IgG-HRP was added. The mixtures were incubated for 1 h, followed by the addition of TMB (100 μL /well). After incubation for 10 min, the absorbance ($A_{650\text{nm}}$) was read with a multifunctional microplate reader (Tecan, Salzburg, Austria). All incubations were carried out on a thermomixer (Eppendorf, Hamburg, Germany) at 37°C and 400 rpm, followed by washing three times with PBST (10 mM PBS containing 0.1% Tween 20, $\text{pH} 7.4$) using a DEM-3 washing machine (Tuopu, Beijing, China).

2.5. Cl-ELISA Establishment

A 100 μL /well OVA-Hapten (5 mg/L) in PBS (10 mM, $\text{pH} 7.4$) was coated on 96-well opaque assay plates for 2 h. The plates were then washed, followed by the addition and incubation of BSA (300 μL /well) blocker for 1 h. After washing, analyte (50 μL /well) dissolved in 10% MeOH–PBS (10 mM, $\text{pH} 7.4$) and antibody (0.5 mg/L, 50 μL /well) diluted with tris (50 mM, $\text{pH} 7.4$) were added and incubated for 2 h on a blocked plate. After washing 3 times, 100 μL /well of diluted (1/1000) goat antimouse IgG-HRP was added. The mixtures were incubated for 1 h, followed by the addition of HRP-chemiluminescent reagents A and B (50 μL /well). After incubation for 3.6 min, the luminescence (total luminescence) was read with a multifunctional microplate reader (Tecan, Salzburg, Austria). All incubations were carried out on a thermomixer (Eppendorf, Hamburg, Germany) at 37°C and 400 rpm, followed by washing three times with PBST (10 mM PBS containing 0.1% Tween 20, $\text{pH} 7.4$) using a DEM-3 washing machine (Tuopu, Beijing, China).

2.6. Calibration Curves

The calibration curve for Cl-ELISA was plotted by considering IMI concentrations on the x-axis against percent inhibition on the y-axis. The percent inhibition was calculated using the following Equation (1) [25,26]. Similarly, the Co-ELISA was calculated using Equation (2).

$$I\% = \left(1 - \frac{RLU_x - RLU_{\min}}{RLU_{\max} - RLU_{\min}}\right) \times 100\% \quad (1)$$

$$I\% = \left(1 - \frac{OD_x - OD_{\min}}{OD_{\max} - OD_{\min}}\right) \times 100\% \quad (2)$$

In Equation (1), RLU_{\max} and RLU_x are the response without IMI and the response value when the concentration of the standard solution is x , respectively. RLU_{\min} is the response value of the blank control.

In Equation (2), OD_{\max} and OD_x are the response without IMI and the response value when the concentration of the standard solution is x , respectively. OD_{\min} is the response value of the blank control.

3. Results

3.1. Optimization Parameters of the Assays

3.1.1. Antigen and Antibody Concentrations

The parameters of the CI-ELISA protocol were optimized according to the chessboard assay, including signal values greater than 5.0×10^5 , high RLU_{\max}/IC_{50} , significant pesticide inhibition effects, and cost savings [24,26]. For CI-ELISA, the maximum value of RLU_{\max}/IC_{50} means a larger detection range and the highest sensitivity for chemiluminescence [27]. As shown in Table 1, a combination of 5 mg/L coated antigen and 0.5 mg/L antibodies were selected in the CI-ELISA system because $R^2 = 0.996$, $RLU_{\max} 6.24 \times 10^6$ was greater than 5.0×10^5 , and cost savings. As shown in Table 1, antibody concentrations that are too high or too low at constant OVA-Hapten concentrations can decrease RLU and lower sensitivity, possibly due to the hook effect [28].

For Co-ELISA, we used a chessboard assay to screen for a combination of antigen–antibody concentrations. $OD = 1$ is used as a target because it can save the amount of antigen and antibody used and meet the method's sensitivity [29,30]. A combination with $OD = 1$ and the smallest antigen–antibody concentration was used as the optimized concentration. As shown in Table 2, the higher the antigen and antibody concentrations were, the greater the OD value. When the antigen concentration was constant, the OD value decreased with increasing antibody dilution (antibody dilutions from 2 to 16 times); the OD value changed without an obvious pattern with increasing antibody dilution (antibody dilutions from 32 to 128 times). Because the concentration of antibodies is too low, the binding rate of antibodies and antigens may be reduced. The combinations of antigens with an antibody with OD values of approximately 1.0 were 20 mg/L with 4 mg/L and 10 mg/L with 2 mg/L, and the combination of 10 mg/L with 2 mg/L was chosen according to cost savings.

3.1.2. Blocking Agent

As a critical step, protein antibodies or antigens are immobilized on plastic surfaces through nonspecific binding in ELISA. Binding nonspecific proteins may lead to a decline in sensitivity and specificity and can also produce false negative results [25]. To avoid nonspecific binding, proteins were used to block the vacant sites in the plastic well. As one of the most commonly used blocking agents, BSA effectively showed optimum results in ELISA [31,32]. Therefore, BSA was chosen as the blocking solution and tested in the 0.5–5% range. According to the results (Figure 2), with increasing BSA concentration, the RLU values of the negative wells decreased continuously. The results showed that as the concentration of BSA increased, the excessive BSA adsorption on the plastic plates hindered the binding of antigens and antibodies. With increasing BSA concentration, as shown in Figure 2, the RLU values of the positive wells decreased and remained unchanged. The results suggest that the low concentration of BSA could not wholly block the adsorption sites of the plastic plates, which quickly produced false negatives. When the N/P value is the maximum, its chemiluminescence value is larger, and the sensitivity is higher. A concentration of 2% BSA was chosen as the blocking concentration.

3.1.3. Methanol

IMI solubility in water is less than that in organic solvents [33], and adding an appropriate amount of organic solvent to the buffer solution assists in the dissolution of IMI. However, an excessively high solvent content might affect the antigen–antibody reaction [34]. To compare the effect of different methanol contents on CI-ELISA, PBS buffers containing 1%, 5%, 10%, 20%, and 30% volumes of methanol were prepared to dilute the standard solutions. The results (Figure 3) show that the RLU of the negative wells decreased with increasing methanol volume from 5% to 30%. This indicates that a high methanol volume affects antigen–antibody reactions. When the volume of methanol was 10%, the chemical RLU of the positive wells was the smallest, and the value of N/P was the largest at 4.6. The PBS buffer containing 10% methanol was selected for the CI-ELISA method

to prepare the standard pesticide solution under the conditions of pesticide solubility, maximum signal value, and detection sensitivity.

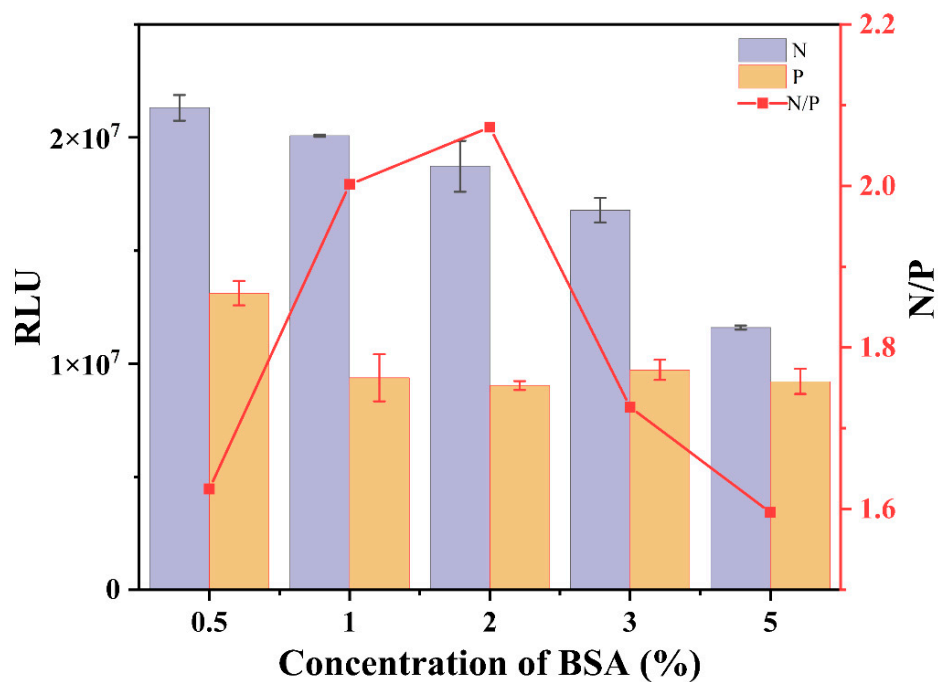


Figure 2. Effects of BSA on CI-ELISA. The data are averages of three replicates. P: the RLU values of the positive wells (the concentration of IMI = 3.125 µg/L), N: the RLU values of the negative wells (the concentration of IMI = 0).

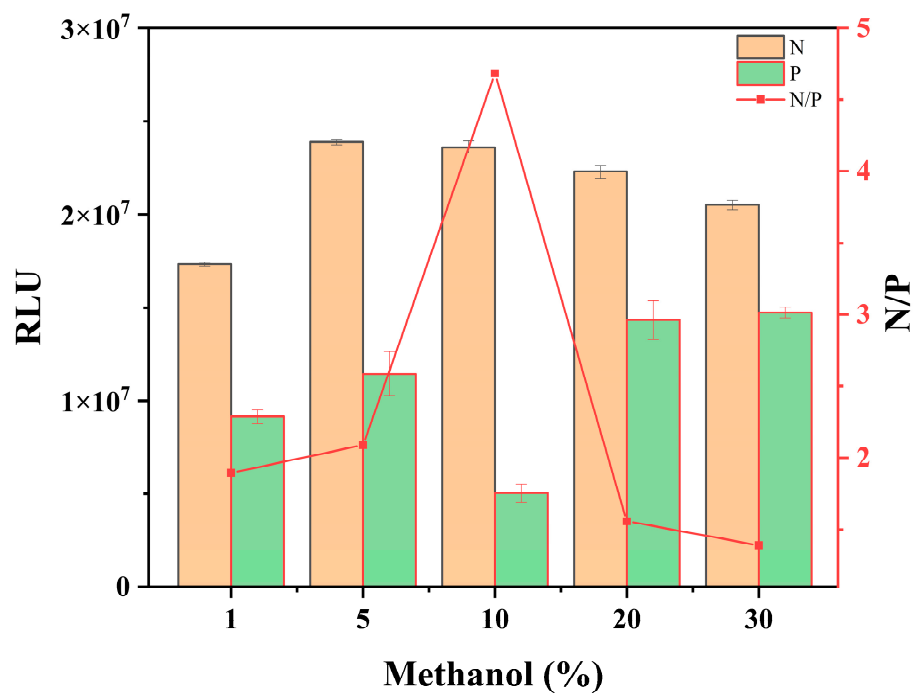


Figure 3. Effects of methanol on CI-ELISA. The data are averages of three replicates. P: the RLU values of the positive wells (the concentration of IMI = 3.125 µg/L), N: the RLU values of the negative wells (the concentration of IMI = 0).

3.1.4. Reaction Time

The substrate action time is an important factor affecting the sensitivity of CI-ELISA. A reaction time that is too short or too long might result in a false negative. The chemiluminescence dynamic curves of the 0-well plates were analyzed under three different matrices to control the reaction time. The results (Figure 4a) showed that the RLU tended to increase and decrease with time. The plateau stabilization period of chemiluminescence (1.8–5.4 min) was approximately 3.6 min. At 3.6 min, the chemiluminescence values reached a maximum in the three matrices: cabbage 2.5×10^7 , cucumber 2.0×10^7 , and zucchini 1.7×10^7 .

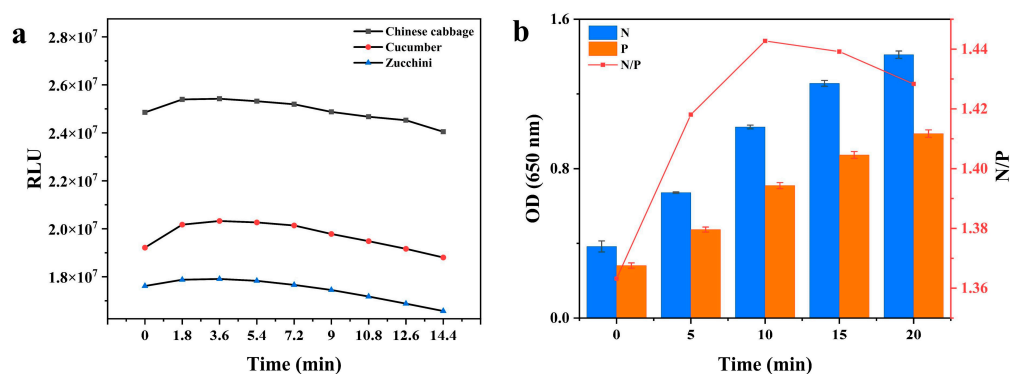


Figure 4. (a) The dynamic curve of CI-ELISA in the three tested vegetable samples from 0 to 14.4 min with no analyte. (b) Absorbance values for optimization of reaction time (0, 5, 10, 15, and 20 min) for Co-ELISA.

Under optimal conditions, Co-ELISA was set at 37°C with substrate action times of 0, 5, 10, 15, and 20 min (Figure 4b). With increasing time, the OD values of the negative and positive wells increased. At 10 min, the OD value was approximately 1.0, and the N/P value was a maximum. Thus, 10 min was chosen as the best action time for the TMB solution. The time of the maximum N/P value was chosen as the optimal action time (10 min) of the TMB solution. The RLU of CI-ELISA could be measured immediately after the addition of the HRP-chemiluminescent reagents (3.6 min), while the colorimetric method required 10 min of reaction.

3.2. Calibration Curves

All these factors were accounted for, and the optimal conditions for CI-ELISA were as follows: coated antigen (5 mg/L) and antibody (0.5 mg/L) produced the highest $\text{RLU}_{\text{max}}/\text{IC}_{50}$ ratio; 10% methanol, 2% BSA, and 3 min substrate action time were used for CI-ELISA. Under optimal conditions, Figure 5a shows the CI-ELISA standard curve for IMI. A calibration curve was obtained based on a similar linear section of the standard curve (inset of Figure 5a). The limit of detection (LOD) and the sensitivity (IC_{50}) of CI-ELISA were $0.19 \mu\text{g/L}$ and $2.66 \mu\text{g/L}$, respectively. Similarly, the optimal conditions for Co-ELISA were as follows: coated antigen (10 mg/L) and antibody (2 mg/L) produced the $\text{OD} = 1$; 10% methanol, 2% BSA, and 10 min substrate action time were used for Co-ELISA. Under optimal conditions, Figure 5b shows the Co-ELISA standard curve for IMI. A calibration curve was obtained based on a similar linear section of the standard curve (inset of Figure 5b). The limit of detection (LOD) and the sensitivity (IC_{50}) of CI-ELISA were $1.56 \mu\text{g/L}$ and $8.15 \mu\text{g/L}$, respectively.

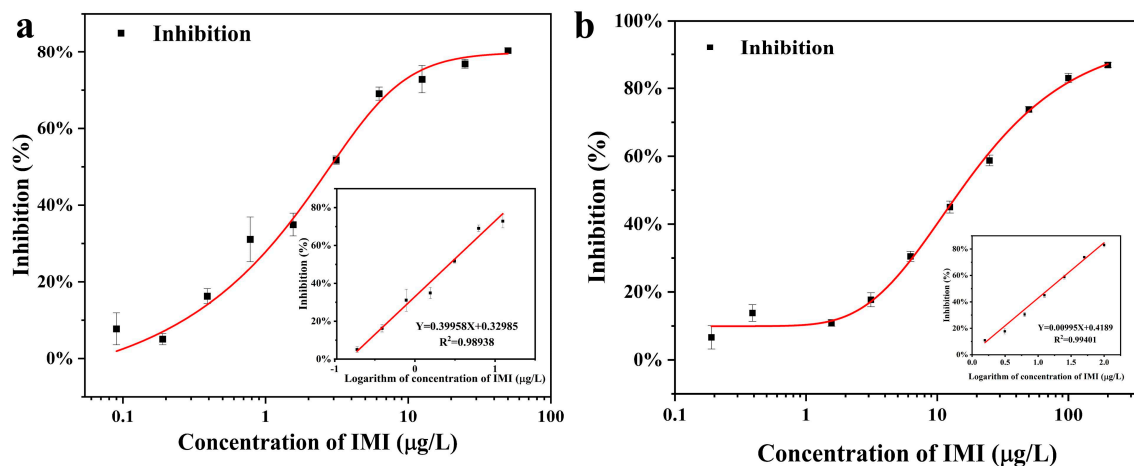


Figure 5. (a) Standard curve for the detection of IMI using CI-ELISA. (b) Standard curve for the detection of IMI using Co-ELISA.

Figure 5 shows the Co-ELISA linearity over a wide range (1.56–200 µg/L) with $R^2 = 0.9893$. In comparison, the CI-ELISA linearity range (0.19–25 µg/L) with $R^2 = 0.9940$ may be caused by the concentration of antigen and antibody of Co-ELISA being greater than that of CI-ELISA. The sensitivity of CI-ELISA ($IC_{50} = 1.56$ µg/L) was greater than that of Co-ELISA ($IC_{50} = 8.15$ µg/L), which may be due to the sensitivity of the chemiluminescence assay compared to that of the colorimetric assay (Table 3). From Table 3, for Co-ELISA, the linearity (1.56–200 µg/L) was broader than that of CI-ELISA (0.19–25 µg/L), which achieved quantitative analysis in two orders of magnitude ranges. For CI-ELISA, the concentration of antigen and antibody was economical compared to Co-ELISA. The IC_{50} (1.56 µg/L) of CI-ELISA was more sensitive than the IC_{50} (8.15 µg/L) of Co-ELISA, which was caused by the chemiluminescence assay being more sensitive than the colorimetric assay. In addition, chemiluminescent assays were time-saving and efficient compared to colorimetric assays.

Table 3. Comparison between CI-ELISA and Co-ELISA.

Parameters	CI-ELISA	Co-ELISA
Antigen (mg/L)	5	10
Antibody (mg/L)	0.5	2
Linearity (µg/L)	0.19–25	1.56–200
R^2	0.9940	0.9893
Reaction time (min)	3.6	10
IC_{50} (µg/L)	1.56	8.15

3.3. Optimization of Sample Preparation

Method 1 was the sample preparation for CI-ELISA and Co-ELISA. Co-ELISA showed good recovery, while CI-ELISA had poor recovery (26.8–237.5%) and RSD (1.4–52.7%) (Table 4). The recovery and RSD of CI-ELISA could not meet the recovery (between 60 and 120%) and RSD ($\leq 30\%$), according to NY/T 788-2018 [35]. Due to the mutual solubility of methanol and water, the proportion of methanol in the extracted supernatant could not be determined, thereby, reducing the sensitive detection of trace IMI in CI-ELISA. Thus, method 1 was optimized by transferring all the supernatant to a centrifuge tube, after which water was added to fix the volume of methanol to 10 mL to ensure a constant volume of methanol. A trace amount of IMI could be extracted completely, making CI-ELISA obtain good recovery.

Table 4. Recovery of spiked IMI in vegetable samples (Chinese cabbage, cucumber, and zucchini) using Co-ELISA and CI-ELISA (n = 3).

Sample	Method 1				Method 1				Method 2			
	Spiked (µg/L)	Co-ELISA (µg/L)	Recovery (%)	RSD (%)	Spiked (µg/L)	CI-ELISA (µg/L)	Recovery (%)	RSD (%)	Spiked (µg/L)	CI-ELISA (µg/L)	Recovery (%)	RSD (%)
Chinese cabbage	10	11.35 ± 1.87	113.5	5.4	5	1.34 ± 0.46	26.8	7.5	5	5.47 ± 0.14	109.3	4.7
	50	58.74 ± 1.94	117.5	6.2	10	5.85 ± 1.13	58.5	5.6	10	7.03 ± 0.11	70.3	1.5
	100	81.71 ± 2.02	81.7	6.9	20	18.19 ± 0.56	91.0	1.4	20	13.94 ± 0.17	69.7	8.1
cucumber	10	8.21 ± 1.14	82.1	0.7	5	5.06 ± 0.04	101.2	8.1	5	4.49 ± 0.69	89.7	7.9
	50	49.11 ± 1.20	98.2	1.7	10	7.23 ± 0.09	72.3	24.0	10	11.41 ± 0.47	114.1	1.0
	100	79.38 ± 1.31	79.4	3.2	20	9.30 ± 0.60	46.5	19.5	20	14.82 ± 0.60	74.1	5.5
zucchini	10	11.11 ± 2.05	111.1	7.9	5	9.35 ± 0.30	187.0	43.8	5	6.07 ± 0.17	120.6	5.0
	50	58.81 ± 2.42	117.6	11.1	10	23.74 ± 0.18	237.5	45.7	10	6.99 ± 0.43	69.9	15.0
	100	82.55 ± 2.50	82.5	11.6	20	27.10 ± 0.19	135.5	52.7	20	19.94 ± 0.24	104.9	8.8

3.4. Accuracy and Precision

The inhibition curves for IMI in Chinese cabbage, cucumber, and zucchini matrices using Co-ELISA and CI-ELISA are shown in Figures 6 and 7. Both Co-ELISA and CI-ELISA achieved quantitative analysis of IMI with high sensitivity. The linearity of Co-ELISA was observed in the range of 3.125 µg/L–100 µg/L in Chinese cabbage ($R^2 = 0.9746$), 1.56 µg/L–200 µg/L in cucumber ($R^2 = 0.9743$), and 1.56 µg/L–200 µg/L in zucchini ($R^2 = 0.9756$). The linearity of CI-ELISA was observed in the range of 0.39 µg/L–25 µg/L in Chinese cabbage with a good regression coefficient (R^2) of 0.9656, 1.56 µg/L–50 µg/L in cucumber ($R^2 = 0.9577$), and 0.39 µg/L–50 µg/L in zucchini ($R^2 = 0.9873$). Chinese cabbage, cucumber, and zucchini were spiked at concentrations of 10, 50, and 100 µg/L for Co-ELISA and concentrations of 5, 10, and 20 µg/L for CI-ELISA. The recovery was performed under optimized conditions and compared with CI-ELISA for its performance. According to Table 4, for Co-ELISA, the recovery of IMI in spiked samples varied from 81.7 to 117.5% in Chinese cabbage (RSD between 5.4 and 6.9%), 79.4 to 98.2% in cucumber (RSD between 0.7 and 3.2%), and 82.5 to 117.6% in zucchini (RSD between 7.9 and 11.6%). For CI-ELISA, recovery varied between 69.7 and 109.3% in Chinese cabbage (RSD between 1.5 and 8.1%), 74.1 and 114.1% in cucumber (RSD between 1.0 and 7.9%), and 69.9 and 120.6% in zucchini (RSD between 5.0 and 15.0%). Comparing the two assays, Co-ELISA showed the best recovery results, where 79.4 to 117.6% was achieved for all samples (Table 4). At a lower concentration of 5 µg/L, CI-ELISA showed better recovery in cucumber than in Chinese cabbage and zucchini, which could be due to matrix effects. According to China's and the EU's pesticide residue limit standards, (the MRL of IMI in Chinese cabbage is 0.2 mg/kg and that of cucumber and zucchini is 1 mg/kg, China) (the MRL of IMI in Chinese cabbage is 0.01 mg/kg and that of cucumber is 0.5 mg/kg, EU) Co-ELISA and CI-ELISA can meet the requirements of rapidly detecting IMI. Co-ELISA and CI-ELISA are suitable to ensure rapid, reliable, and sensitive detection of IMI in Chinese cabbage, cucumber, and zucchini samples.

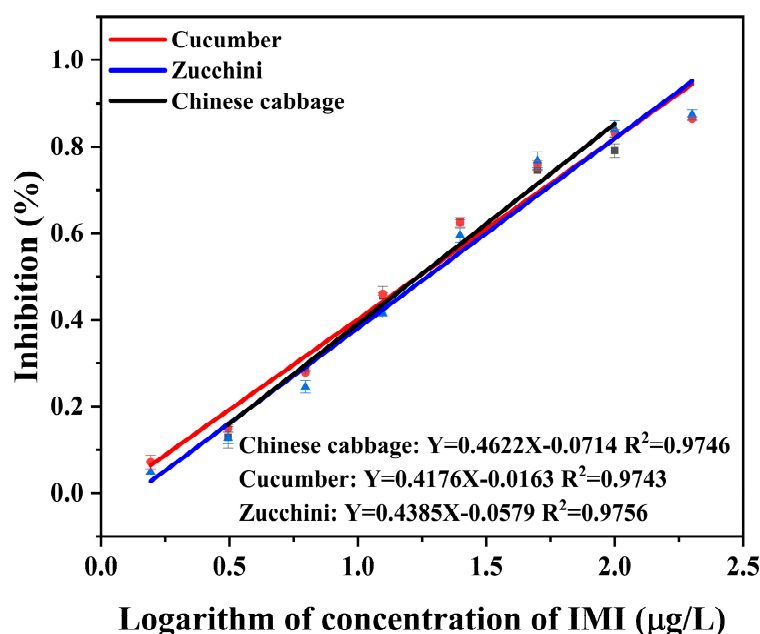


Figure 6. Standard curve for the detection of IMI in vegetable samples (Chinese cabbage, cucumber, and zucchini) using Co-ELISA.

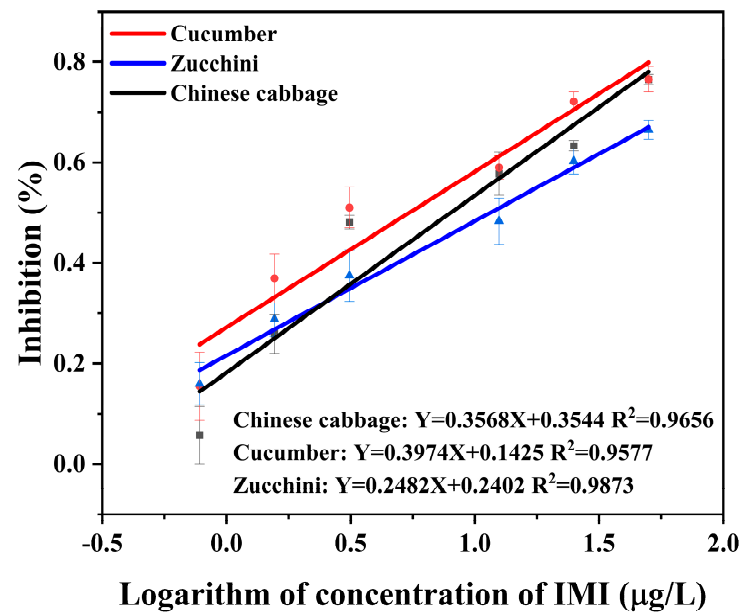


Figure 7. Standard curve for the detection of IMI in vegetable samples (Chinese cabbage, cucumber, and zucchini) using CI-ELISA.

3.5. Comparison with Other Methods for Detecting IMI

Table 5 shows the LOD and linear range of different instruments for detecting IMI. The LOD = 1.56 µg/L of Co-ELISA and the LOD = 0.19 µg/L of CI-ELISA were lower than those of HPLC and HPLC—MS/MS in Table 5, which proved that Co-ELISA and CI-ELISA were feasible. Some immunoassay methods detect IMI with significantly lower LODs than this work and show better results. For example, Wang et al. [36] used an immunochromatographic method based on scandium-tetrakis (4-carboxyphenyl) porphyrin (TCPP) metal–organic framework nanocubes to detect IMI in vegetables, and the Sc-TCPP 3D MOF had good biocompatibility and optical properties, thus, enhancing the sensitivity of the detection. In addition, Fernández et al. [37] constructed an immunosensor for the detection of IMI based on nanogold electrodes and obtained a low LOD of 22 pmol/L. Guo et al. [38] established immunoassay based on graphene oxide (GO) and up-converting nanoparticles (UCNPs) showed a wide detection range of 0.08–50 ng/mL to IMI. The combination of immunoassays and nanomaterials allows for more sensitive detection.

Table 5. Comparison of instruments detecting IMI (n = 3).

Methods	LOD (µg/L)	Recovery (%)	Sample	RSD (%)	Reference
HPLC—MS/MS	5.9	70.1–119.3	fruits	2.7–12.4	[39]
HPLC	2.7	88.9–93.9	juice	3.2–4.1	[40]
HPLC	10	83.3–90.8	soil	2.4–4.4	[41]
HPLC—MS/MS	2.1	85.9–103.8	vegetable	2.6–12.1	[42]
HPLC	8.53	88.9–90.2	vegetable	5.5–6.8	[43]
ITS	0.04	80.0–124.0	vegetable	0.1–2.7	[36]
Immunoassay (UCNPs/GO)	0.08	76.8–101.8	Water, vegetable, tea, honey	-	[38]
Co-ELISA	1.56	79.4–117.6	vegetable	0.7–11.6	This work
CI-ELISA	0.19	69.7–120.6	vegetable	1.0–15.0	

ITS: immunochromatographic test strip; reprinted/adapted with permission from Refs. [36,38]. Copyright 2022, Elsevier; reprinted/adapted with permission from Ref. [41]. Copyright 2022, IOP science; reprinted/adapted with permission from Ref. [43]. Copyright 2022, Taylor & Francis; reprinted/adapted with permission from Chinese Refs. [39,40,42].

4. Conclusions

Herein, Co-ELISA and Cl-ELISA were developed for detecting IMI in Chinese cabbage, cucumber, and zucchini. The recoveries ranged from 81.7 to 117.6% for Co-ELISA and 69.7 to 120.6% for Cl-ELISA. The principle of detection used for both assays can also be applied to detect IMI at a sensitive level in other vegetable samples. Co-ELISA exhibited a wide linear range (1.56–200 µg/L) suitable for IMI testing at the microgram level. Compared with Co-ELISA, Cl-ELISA showed higher sensitivity ($IC_{50} = 2.66$ µg/L), benefiting the trace detection level, which was one order of magnitude higher than that of Co-ELISA. Cl-ELISA is a cost-saving alternative to Co-ELISA in terms of the amount of antigen and antibody used and detection time. This study builds colorimetric and chemiluminescent assays based on ELISA detection of IMI and provides the theoretical basis for selecting an optical detection assay.

Author Contributions: Conceptualization, R.Z. and G.C.; methodology, G.L.; software, X.H.; validation, X.X., X.H. and G.C.; formal analysis, G.C.; investigation, L.L.; resources, Y.Z.; data curation, G.C.; writing—original draft preparation, R.Z. and G.C.; writing—review and editing, G.C. and A.M.A.; visualization, X.X.; supervision, D.X.; project administration, X.H.; funding acquisition, D.X. All authors have read and agreed to the published version of the manuscript.

Funding: This study was financially supported by the Agricultural Science and Technology Innovation Program of CAAS (CAAS-ZDRW202011, CAAS-TCX2019025-5), the China Agriculture Research System of MOF and MARA (CARS-23-E03), and the National Key Research Development Program of China (2020YFD1000300).

Data Availability Statement: The original contributions presented in this study are included in the article, and further inquiries can be directed to the corresponding authors.

Conflicts of Interest: The authors declare no conflict of interest.

References

1. Zhai, R.; Zhang, K.; Chen, G.; Liu, G.; Huang, X.; Gao, M.; Zhou, J.; Xu, X.; Li, L.; Zhang, Y.; et al. Residue, Dissipation Pattern, and Dietary Risk Assessment of Imidacloprid in Chinese Chives. *Front. Nutr.* **2022**, *9*, 846333. [[CrossRef](#)] [[PubMed](#)]
2. Yang, L.; Shen, Q.; Zeng, T.; Li, J.; Li, W.; Wang, Y. Enrichment of imidacloprid and its metabolites in lizards and its toxic effects on gonads. *Environ. Pollut.* **2020**, *258*, 113748. [[CrossRef](#)] [[PubMed](#)]
3. Seifrtova, M.; Halesova, T.; Sulcova, K.; Riddellova, K.; Erban, T. Distributions of imidacloprid, imidacloprid-olefin and imidacloprid-urea in green plant tissues and roots of rapeseed (*Brassica napus*) from artificially contaminated potting soil. *Pest Manag. Sci.* **2017**, *73*, 1010–1016. [[CrossRef](#)] [[PubMed](#)]
4. Van Loon, S.; Vicente, V.B.; van Gestel, C.A.M. Long-Term Effects of Imidacloprid, Thiacloprid, and Clothianidin on the Growth and Development of *Eisenia andrei*. *Environ. Toxicol. Chem.* **2022**, *41*, 1686–1695. [[CrossRef](#)]
5. Sriapha, C.; Trakulsrichai, S.; Tongpoo, A.; Pradoo, A.; Rittilert, P.; Wananukul, W. Acute Imidacloprid Poisoning in Thailand. *Ther. Clin. Risk Manag.* **2020**, *16*, 1081–1088. [[CrossRef](#)]
6. Du, M.; Yang, Q.; Liu, W.; Ding, Y.; Chen, H.; Hua, X.; Wang, M. Development of immunoassays with high sensitivity for detecting imidacloprid in environment and agro-products using phage-borne peptides. *Sci. Total Environ.* **2020**, *723*, 137909. [[CrossRef](#)] [[PubMed](#)]
7. Rancan, M.; Sabatini, A.G.; Achilli, G.; Galletti, G.C. Determination of Imidacloprid and metabolites by liquid chromatography with an electrochemical detector and post column photochemical reactor. *Anal. Chim. Acta* **2006**, *555*, 20–24. [[CrossRef](#)]
8. Iwafune, T.; Ogino, T.; Watanabe, E. Water-based extraction and liquid chromatography-tandem mass spectrometry analysis of neonicotinoid insecticides and their metabolites in green pepper/tomato samples. *J. Agric. Food Chem.* **2014**, *62*, 2790–2796. [[CrossRef](#)]
9. Lodevico, R.G.; Li, Q.X. Determination of Total Imidacloprid Residues in Coffee by Gas Chromatography–Mass Spectrometry. *Analytical Letters*. **2002**, *35*, 315–326. [[CrossRef](#)]
10. Zhai, R.; Chen, G.; Liu, G.; Huang, X.; Xu, X.; Li, L.; Zhang, Y.; Wang, J.; Jin, M.; Xu, D.; et al. Enzyme inhibition methods based on Au nanomaterials for rapid detection of organophosphorus pesticides in agricultural and environmental samples: A review. *J. Adv. Res.* **2022**, *37*, 61–74. [[CrossRef](#)]
11. Li, H.; Jin, R.; Kong, D.; Zhao, X.; Liu, F.; Yan, X.; Lin, Y.; Lu, G. Switchable fluorescence immunoassay using gold nanoclusters anchored cobalt oxyhydroxide composite for sensitive detection of imidacloprid. *Sens. Actuators B Chem.* **2019**, *283*, 207–214. [[CrossRef](#)]
12. Perez-Fernandez, B.; Mercader, J.V.; Checa-Orrego, B.I.; de la Escosura-Muniz, A.; Costa-Garcia, A. A monoclonal antibody-based immunosensor for the electrochemical detection of imidacloprid pesticide. *Analyst* **2019**, *144*, 2936–2941. [[CrossRef](#)] [[PubMed](#)]

13. Bor, G.; Man, E.; Ugurlu, O.; Ceylan, A.E.; Balaban, S.; Durmus, C.; Pinar Gumus, Z.; Evran, S.; Timur, S. in vitro Selection of Aptamer for Imidacloprid Recognition as Model Analyte and Construction of a Water Analysis Platform. *Electroanalysis* **2020**, *32*, 1922–1929. [[CrossRef](#)]
14. Wang, S.H.; Lo, S.C.; Tung, Y.J.; Kuo, C.W.; Tai, Y.H.; Hsieh, S.Y.; Lee, K.L.; Hsiao, S.R.; Sheen, J.F.; Hsu, J.C.; et al. Multichannel nanoplasmonic platform for imidacloprid and fipronil residues rapid screen detection. *Biosens. Bioelectron.* **2020**, *170*, 112677. [[CrossRef](#)]
15. Zhang, W.; Liu, C.; Han, K.; Wei, X.; Xu, Y.; Zou, X.; Zhang, H.; Chen, Z. A signal on-off ratiometric electrochemical sensor coupled with a molecular imprinted polymer for selective and stable determination of imidacloprid. *Biosens. Bioelectron.* **2020**, *154*, 112091. [[CrossRef](#)]
16. Li, H.; He, S.; Liu, G.; Li, C.; Ma, Z.; Zhang, X. Residue and dissipation kinetics of toosendanin in cabbage, tobacco and soil using IC-ELISA detection. *Food Chem.* **2021**, *335*, 127600. [[CrossRef](#)]
17. Watanabe, E.; Miyake, S.; Yogo, Y. Review of enzyme-linked immunosorbent assays (ELISAs) for analyses of neonicotinoid insecticides in agro-environments. *J. Agric. Food Chem.* **2013**, *61*, 12459–12472. [[CrossRef](#)]
18. Zhang, Z.; Chen, Q.; Huang, H.; Zhang, K.; Bai, L.; Tan, G. Ultrasensitive Immunoassay for the Determination of Imidacloprid in Medicinal Herbs. *Anal. Lett.* **2022**, 1–13. [[CrossRef](#)]
19. Watanabe, E.; Baba, K.; Eun, H.; Miyake, S. Application of a commercial immunoassay to the direct determination of insecticide imidacloprid in fruit juices. *Food Chem.* **2007**, *102*, 745–750. [[CrossRef](#)]
20. Zhang, L.; Wang, Z.; Wen, Y.; Shi, J.; Wang, J. Simultaneous detection of parathion and imidacloprid using broad-specificity polyclonal antibody in enzyme-linked immunosorbent assay. *Anal. Methods* **2015**, *7*, 205–210. [[CrossRef](#)]
21. Yue, Y.; Chen, J.; Zhang, M.; Yin, Y.; Dong, Y. Determination of Organophosphorus Pesticides in Vegetables and Fruit by an Indirect Competitive Enzyme-Linked Immunosorbent Assay (ic-ELISA) and a Lateral-Flow Immunochromatographic (LFIC) Strip Assay. *Anal. Lett.* **2022**, *55*, 1701–1718. [[CrossRef](#)]
22. Girotti, S.; Maiolini, E.; Ghini, S.; Eremin, S.; Mañes, J. Quantification of Imidacloprid in Honeybees: Development of a Chemiluminescent ELISA. *Anal. Lett.* **2010**, *43*, 466–475. [[CrossRef](#)]
23. Hu, Y.M.; Feng, H.W.; Liu, S.; Liu, C.; Zhao, P.Y.; Zhang, M.; Zhang, L.; Zhao, J.; Li, J.Z.; Yu, X.M.; et al. The preparation of polyclonal antibody against chlordimeform and establishment of detection by indirect competitive ELISA. *J. Environ. Sci. Health B* **2022**, *57*, 114–124. [[CrossRef](#)] [[PubMed](#)]
24. Tan, W.M.; He, S.P.; Zhang, L.; Zhao, H.W.; Zhao, J.; Li, Z.; Li, X.F.; Wang, B.M. Systematic optimization of antibody and coating antigen concentrations in enzyme linked immunosorbent assay checkerboard assay. *Chin. J. Anal. Chem.* **2008**, *36*, 1191–1195.
25. Mukherjee, M.; Nandhini, C.; Bhatt, P. Colorimetric and chemiluminescence based enzyme linked apta-sorbent assay (ELASA) for ochratoxin A detection. *Spectrochim. Acta A Mol. Biomol. Spectrosc.* **2021**, *244*, 118875. [[CrossRef](#)]
26. Zou, R.B.; Liu, Y.; Wang, S.J.; Zhang, Y.; Guo, Y.R.; Zhu, G.N. Development and evaluation of chemiluminescence enzyme-linked immunoassay for residue detection of three organophosphorus pesticides. *Chin. J. Pestic. Sci.* **2017**, *19*, 37–45.
27. Ding, Y.; Hua, X.; Sun, N.; Yang, J.; Deng, J.; Shi, H.; Wang, M. Development of a phage chemiluminescent enzyme immunoassay with high sensitivity for the determination of imidaclothiz in agricultural and environmental samples. *Sci. Total Environ.* **2017**, *609*, 854–860. [[CrossRef](#)]
28. Shin, S.; Choi, M.; Shim, J.; Park, S. Hook effect detection and detection-range-controllable one-step immunosensor for inflammation monitoring. *Sens. Actuators B Chem.* **2020**, *304*, 127408. [[CrossRef](#)]
29. Song, G.; Huang, L.; Huang, Y.; Liu, W.; Wang, M.; Hua, X. Electrofusion preparation of anti-triazophos monoclonal antibodies for development of an indirect competitive enzyme-linked immunosorbent assay. *J. Immunol. Methods* **2022**, *500*, 113184. [[CrossRef](#)]
30. Parra, J.; Mercader, J.V.; Agullo, C.; Abad-Somovilla, A.; Abad-Fuentes, A. Generation of anti-azoxystrobin monoclonal antibodies from regioisomeric haptens functionalized at selected sites and development of indirect competitive immunoassays. *Anal. Chim. Acta* **2012**, *715*, 105–112. [[CrossRef](#)]
31. Ma, H.; Xu, Y.; Li, Q.X.; Xu, T.; Wang, X.; Li, J. Application of enzyme-linked immunosorbent assay for quantification of the insecticides imidacloprid and thiamethoxam in honey samples. *Food Addit. Contam. Part A.* **2009**, *26*, 713–718. [[CrossRef](#)]
32. Liu, Z.; Liu, J.; Wang, K.; Li, W.; Shelver, W.L.; Li, Q.X.; Li, J.; Xu, T. Selection of phage-displayed peptides for the detection of imidacloprid in water and soil. *Anal. Biochem.* **2015**, *485*, 28–33. [[CrossRef](#)] [[PubMed](#)]
33. Kong, M.Z.; Shi, X.H.; Cao, Y.C.; Zhou, C.R. Solubility of Imidacloprid in Different Solvents. *J. Chem. Eng. Data* **2008**, *53*, 615–618. [[CrossRef](#)]
34. Gui, W.J.; Liu, Y.H.; Wang, C.M.; Liang, X.; Zhu, G.N. Development of a direct competitive enzyme-linked immunosorbent assay for parathion residue in food samples. *Anal. Biochem.* **2009**, *393*, 88–94. [[CrossRef](#)] [[PubMed](#)]
35. Fu, Y.; Wang, Q.; Zhang, L.; Ling, S.; Jia, H.; Wu, Y. Dissipation, occurrence, and risk assessment of 12 pesticides in *Dendrobium officinale* Kimura et Migo. *Ecotoxicol. Environ. Saf.* **2021**, *222*, 112487. [[CrossRef](#)] [[PubMed](#)]
36. Wang, Y.; Zhang, M.; Bu, T.; Bai, F.; Zhao, S.; Cao, Y.; He, K.; Wu, H.; Xi, J.; Wang, L. Immunochromatographic Assay based on Sc-TCPP 3D MOF for the rapid detection of imidacloprid in food samples. *Food Chem.* **2023**, *401*, 134131. [[CrossRef](#)] [[PubMed](#)]
37. Perez-Fernandez, B.; Mercader, J.V.; Abad-Fuentes, A.; Checa-Orrego, B.I.; Costa-Garcia, A.; Escosura-Muniz, A. Direct competitive immunosensor for Imidacloprid pesticide detection on gold nanoparticle-modified electrodes. *Talanta* **2020**, *209*, 120465. [[CrossRef](#)]

38. Guo, Y.; Zou, R.; Si, F.; Liang, W.; Zhang, T.; Chang, Y.; Qiao, X.; Zhao, J. A sensitive immunoassay based on fluorescence resonance energy transfer from up-converting nanoparticles and graphene oxide for one-step detection of imidacloprid. *Food Chem.* **2021**, *335*, 127609. [[CrossRef](#)] [[PubMed](#)]
39. Liang, X.; Zhang, W.Y.; Zhang, W. Simultaneous Determination of Residues of 38 Pesticides in Fruits by QuEChERS Combined with High Performance Liquid Chromatography-Tandem Mass Spectrometry. *Food Sci.* **2020**, *41*, 288–296.
40. Tursen, J.; Yang, T.; Bai, L.; Tan, R. Determination of imidacloprid and acetamiprid in grenadine juice by vortex-assisted dispersive liquid-liquid microextraction coupled with HPLC. *Chin. J. Anal. Lab.* **2019**, *38*, 815–818.
41. Xue, Q.H.; Huang, Q.; Sun, X.H. Effects of Spent Mushroom Compost on Degradation of Imidacloprid in Soil and Plant. *IOP Conf. Ser. Earth Environ. Sci.* **2019**, *252*, 052042. [[CrossRef](#)]
42. Liu, J.G.; Sun, H.; Cheng, X.; Yang, J.; Hou, Z.G. Determination of Paclobutrazol and Other Four Pesticides in the Vegetable by HPLC-MS/MS. *Agrochemicals* **2012**, *51*, 358–363.
43. Badawy, M.E.I.; Ismail, A.M.E.; Ibrahim, A.I.H. Quantitative analysis of acetamiprid and imidacloprid residues in tomato fruits under greenhouse conditions. *J. Environ. Sci. Health B* **2019**, *54*, 898–905. [[CrossRef](#)] [[PubMed](#)]

Disclaimer/Publisher’s Note: The statements, opinions and data contained in all publications are solely those of the individual author(s) and contributor(s) and not of MDPI and/or the editor(s). MDPI and/or the editor(s) disclaim responsibility for any injury to people or property resulting from any ideas, methods, instructions or products referred to in the content.